Supplementary Information (SI) for Journal of Materials Chemistry B.

Modulating the Anti-Cancer Photodynamic Efficiency of Molybdenum-Iodide Nanoclusters via Ligand Design

Tomáš Přibyl,[a,b*] Karel Škoch,[b] Dmytro Bavol,[b] Ivana Křížová,[c] Jaroslav Zelenka,[a] Tomáš Ruml,[a] Kamil Lang[b] and Kaplan Kirakci[b*]

[a] *Department of Biochemistry and Microbiology, University of Chemistry and Technology Prague, Technická 5, 166 28 Praha 6, Czech Republic.*

[b] *Institute of Inorganic Chemistry of the Czech Academy of Sciences, Řež 1001, 250 68 Husinec-Řež, Czech Republic.*

[c] *Department of Biotechnology, University of Chemistry and Technology Prague, Technická 5, 166 28 Praha 6, Czech Republic.*

Content

Figure S1. ^{1}H NMR (d_6-DMSO, 600 MHz, 293K) spectrum of 11,12-didehydro-oxodibenz[b,f]azocine-5(6H)-hexanoic acid.

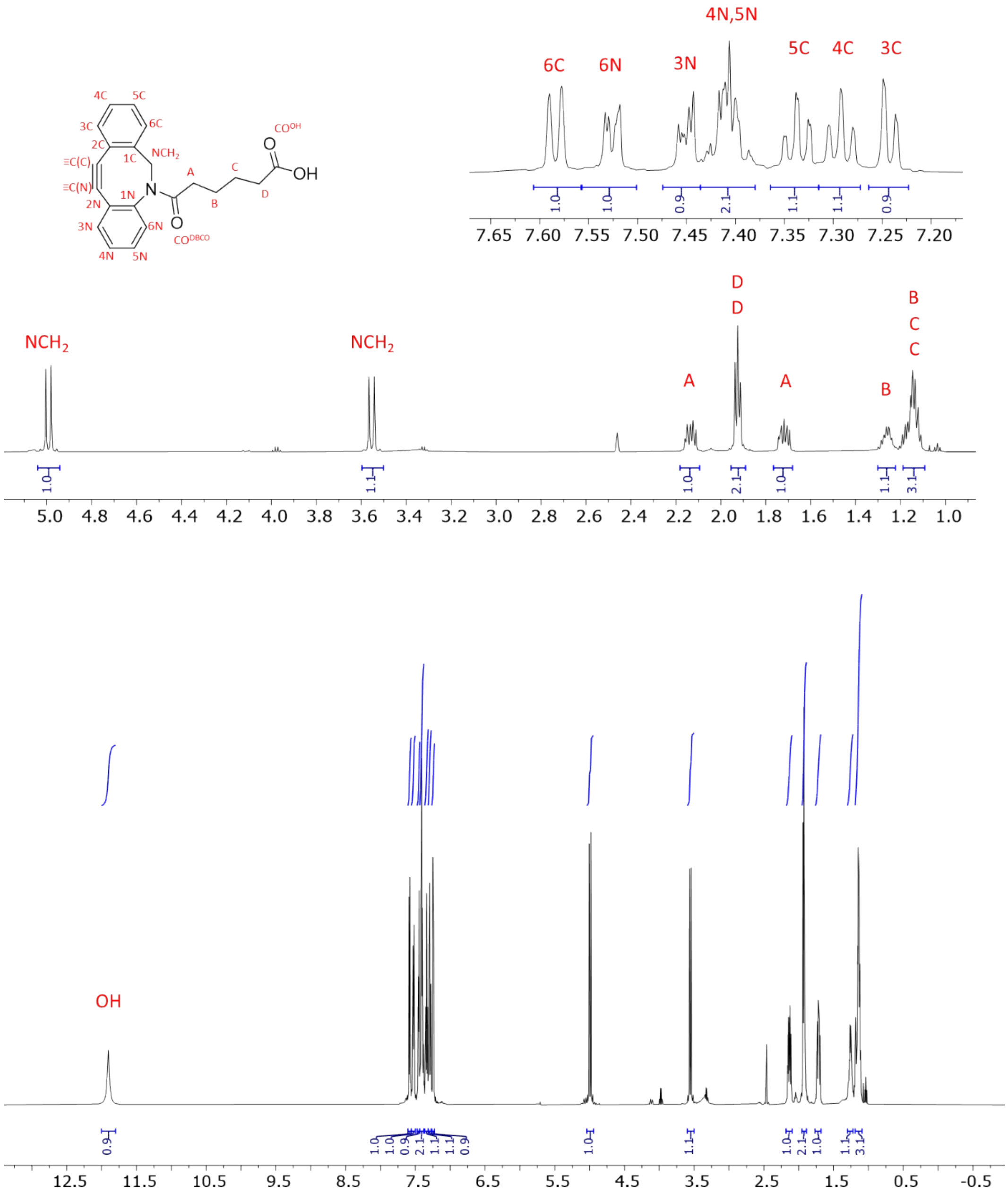

^{1}H NMR (d_6-DMSO, 600 MHz, 293 K): 11.94 (br, 1H, COOH), [7.62 ($^3J_{HH}$ = 7.5 Hz, 1H, CH^{6C}), 7.56 (m, 1H, CH^{6N}), 7.49 (m, 1H, CH^{3N}), 7.45-7.43 (m, 2H, CH^{4N+5N}), 7.38 (dd, $^3J_{HH}$ = $^3J_{HH}$ = 7.5 Hz, 1H, CH^{5C}), 7.33 (dd, $^3J_{HH}$ = $^3J_{HH}$ = 7.5 Hz, 1H, CH^{4C}), 7.28 (d, $^3J_{HH}$ = 7.5 Hz, 1H, CH^{3C})](CH^{Ar}), [5.03 (d, $^2J_{HH}$ = 14.1 Hz), 3.59 (d, $^2J_{HH}$ = 14.1 Hz)](each 1H, CH$_2$N), 2.17 (ddd, $^2J_{HH}$ = 15.7 Hz, $^3J_{HH}$ = 7.9 Hz, $^3J_{HH}$ = 6.2 Hz, 1H, CH$_2$^{A}), 1.96 (m, 2H, CH$_2$^{D}), 1.76 (ddd, $^2J_{HH}$ = 15.7 Hz, $^3J_{HH}$ = 8.3 Hz, $^3J_{HH}$ = 6.1 Hz, 1H, CH$_2$^{A}), 1.30 (m, 1H CH$_2$^{B}), 1.20 (m, 1H CH$_2$^{B}), 1.18 (m, 2H CH$_2$^{C}).

Figure S2. $^{13}C\{^{1}H\}$ NMR (d_6-DMSO, 151 MHz, 293 K) spectrum of 11,12-didehydro-oxodibenz[b,f]azocine-5(6H)-hexanoic acid.

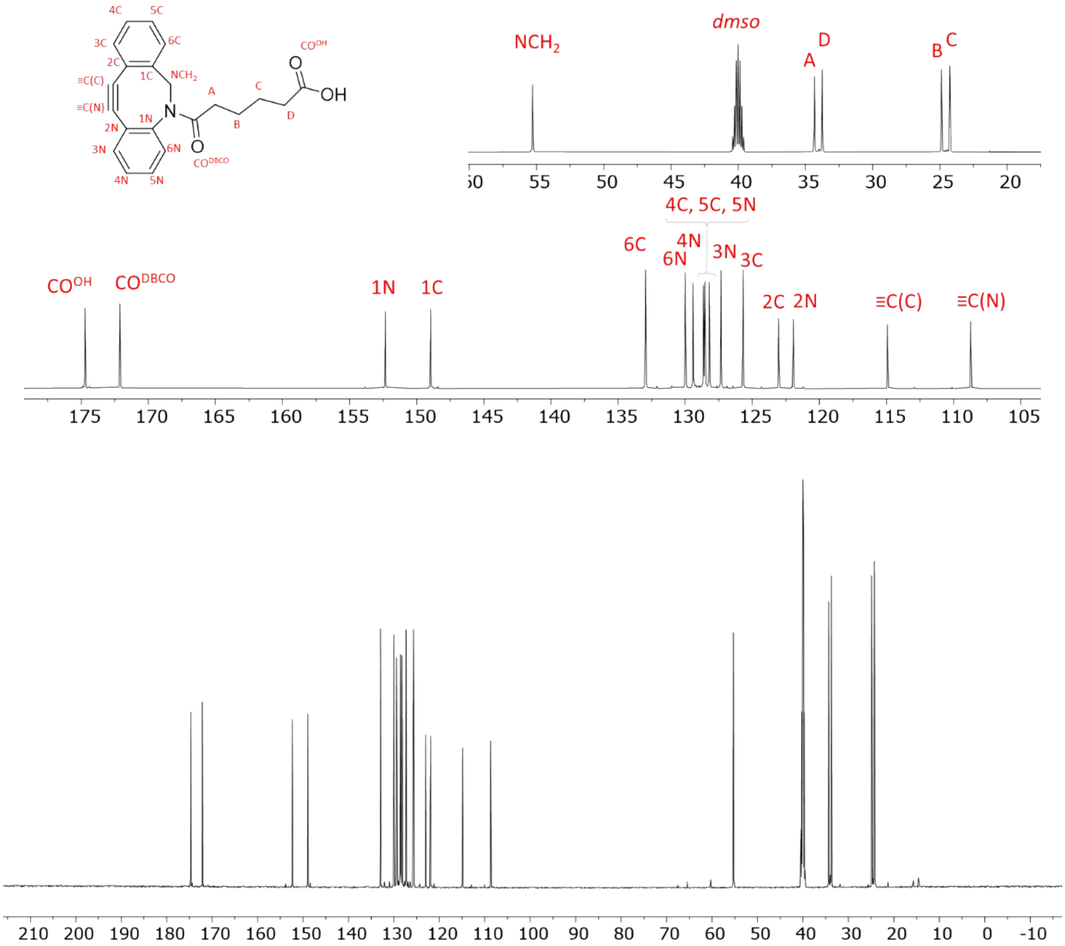

$^{13}C\{^{1}H\}$ NMR (d_6-DMSO, 151 MHz, 293 K): 174.2 (COOH), 171.6 (CO-amide), 151.9 (C^{1N}), 148.5 (C^{1C}), 132.5 (CH^{6C}), 129.5 (CH^{6N}), 128.9 (CH^{4N}), [128.2, 128.1, 127.7](CH^{4C}, CH^{5C}, CH^{5N}), 126.8 (CH^{3N}), 125.2 (CH^{3C}), 122.5 (C^{2C}), 121.5 (C^{2N}), 114.4 (≡C(C)), 108.2 (≡C(N)), 54.8 (NCH_2^{DBCO}), 33.8 (CH_2^{A}), 33.3 (CH_2^{D}), 24.4 (CH_2^{B}), 23.8 (CH_2^{C}).

Figure S3. ^{1}H NMR (d_6-DMSO, 600 MHz, 293K) spectrum of **1**.

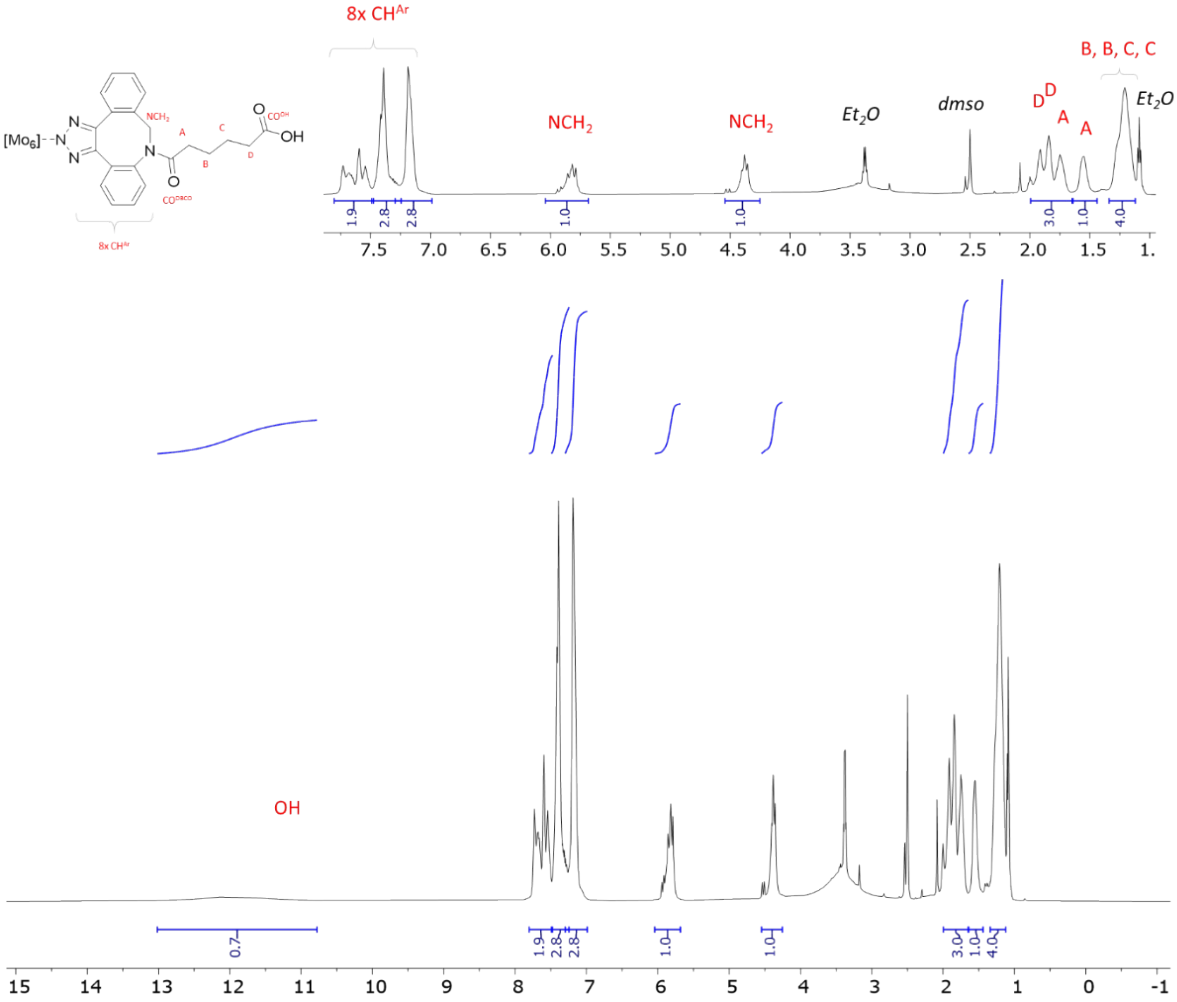

^{1}H NMR (d_6-DMSO, 600 MHz, 293 K): 11.95 (br, 1H, COOH), 7.77-7.10 (m, 8H, CH^{Ar}), 5.82 (m, 1H, NCH_2), 4.73 (m, 1H, NCH_2), 1.91 (m, 1H, CH_2^D), 1.83 (m, 1H, CH_2^D), 1.74 (m, 1H, CH_2^A), 1.56 (m, 1H, CH_2^A), 1.32-1.09 (m, 4H, CH_2^B and CH_2^C).

Figure S4. ^{13}C{^{1}H} NMR (d_6-DMSO, 151 MHz, 293 K) spectrum of **1**.

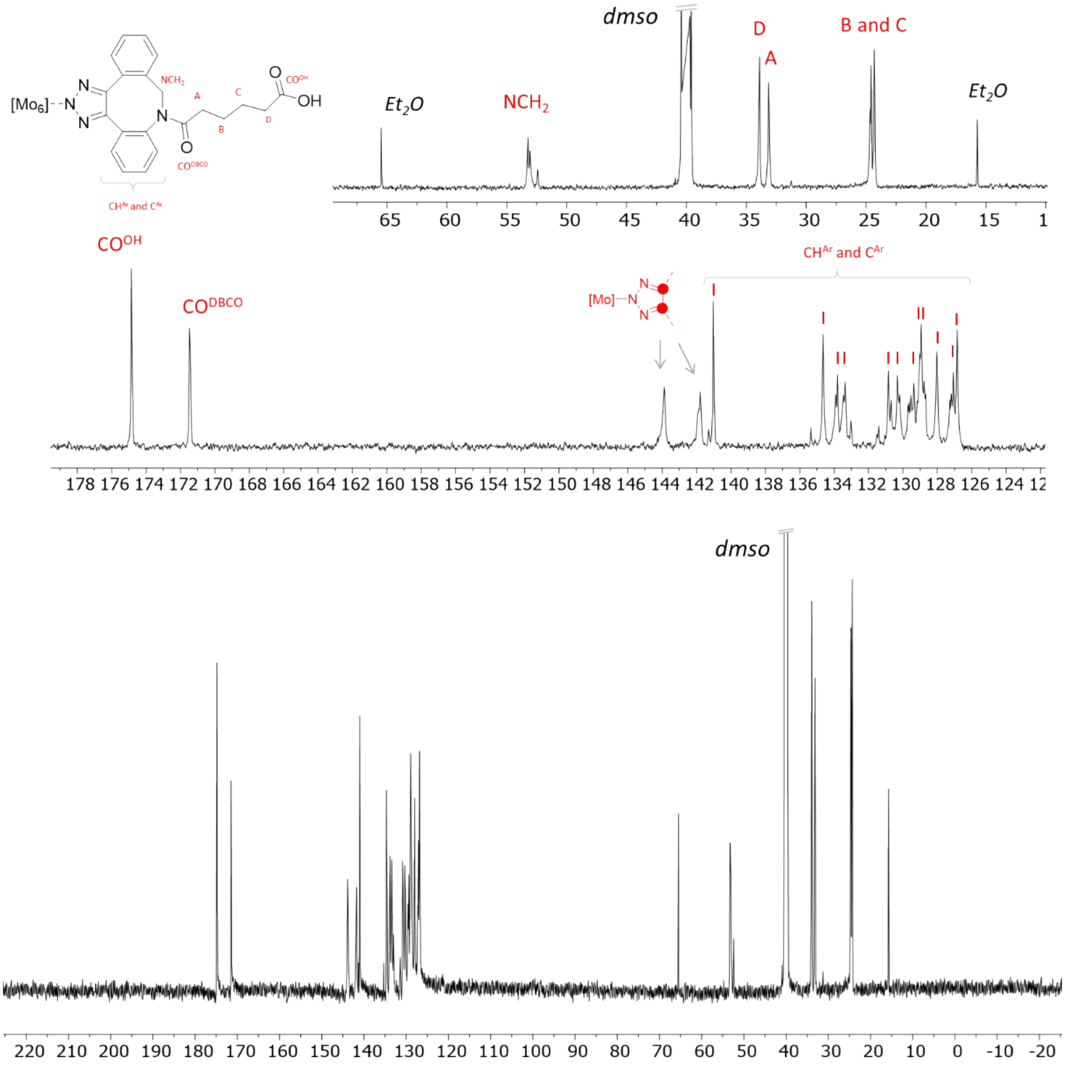

^{13}C{^{1}H} NMR (d_6-DMSO, 151 MHz, 293 K): 174.8 (COOH), 171.5 (CO-amide), [143.9, 141.8](C-triazole), [141.0, 134.6, 133.8, 133.4, 130.9, 130.3, 129.4, 128.9, 128.8, 128.0, 127.1, 126.8](C^{Ar} and CH^{Ar}), 53.2 ($NCH2^{DBCO}$), 33.9 (CH_2^{D}), 33.1 (CH_2^{A}), 24.6 ($CH_2^{B\text{ or }C}$), 24.3 ($CH_2^{B\text{ or }C}$).

Figure S5. ^{1}H NMR (d_6-DMSO, 600 MHz, 293K) spectrum of 3-amino-1-(11,12-didehydrodibenz[b,f]azocin-5(6H)-yl)-1-propanone.

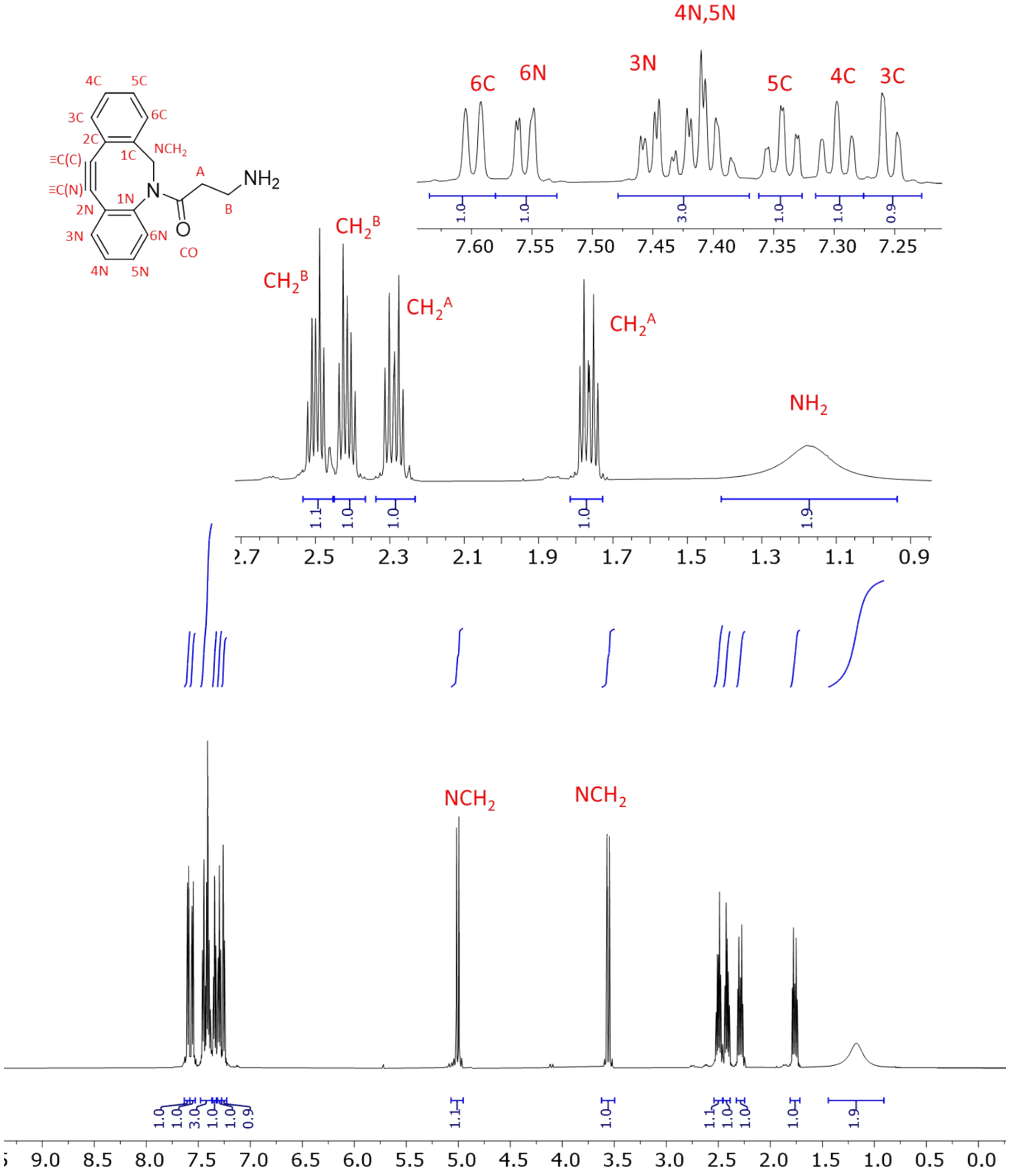

^{1}H NMR (d_6-DMSO, 600 MHz, 293 K): [7.60 (d, $^3J_{HH}$ = 7.6 Hz, 1H, CH^{6C}), 7.56 (dd, $^3J_{HH}$ = 7.4 Hz, $^4J_{HH}$ = 1.3 Hz, 1H, CH^{6N}), 7.45 (dd, $^3J_{HH}$ = 6.9 Hz, $^4J_{HH}$ = 1.6 Hz, 1H, CH^{3N}), 7.41 (m, 2H, CH^{4N} and CH^{5N}), 7.34 (ddd, $^3J_{HH} \approx ^3J_{HH} \approx$ 7.5 Hz, $^4J_{HH}$ = 1.3 Hz, 1H, CH^{5C}), 7.30 (ddd $^3J_{HH} \approx ^3J_{HH} \approx$ 7.4 Hz, $^4J_{HH}$ = 1.3 Hz, 1H, CH^{4C}), 7.25 (dd, $^3J_{HH}$ = 7.5 Hz, $^4J_{HH}$ = 1.3 Hz, 1H, CH^{3C})](CH^{Ar}), [5.01 (d, $^2J_{HH}$ = 14.1 Hz), 3.56 (d, $^2J_{HH}$ = 14.1 Hz)](CH$_2$N), 2.50 (dt, $^2J_{HH}$ = 13.2 Hz, $^3J_{HH}$ = 6.8 Hz, 1H, CH$_2^B$), 2.41 (dt, $^2J_{HH}$ = 13.2 Hz, $^3J_{HH}$ = 6.6 Hz), 2.29 (dt, $^2J_{HH}$ = 15.5 Hz, $^3J_{HH}$ = 6.8 Hz, CH$_2^A$), 1.76 (dt, $^2J_{HH}$ = 15.5 Hz, $^3J_{HH}$ = 6.7 Hz, CH$_2^A$), 1.17 (br, 2H, NH$_2$).

Figure S6. $^{13}C\{^1H\}$ NMR (d_6-DMSO, 151 MHz, 293 K) spectrum of 3-amino-1-(11,12-didehydrodibenz[b,f]azocin-5(6H)-yl)-1-propanone.

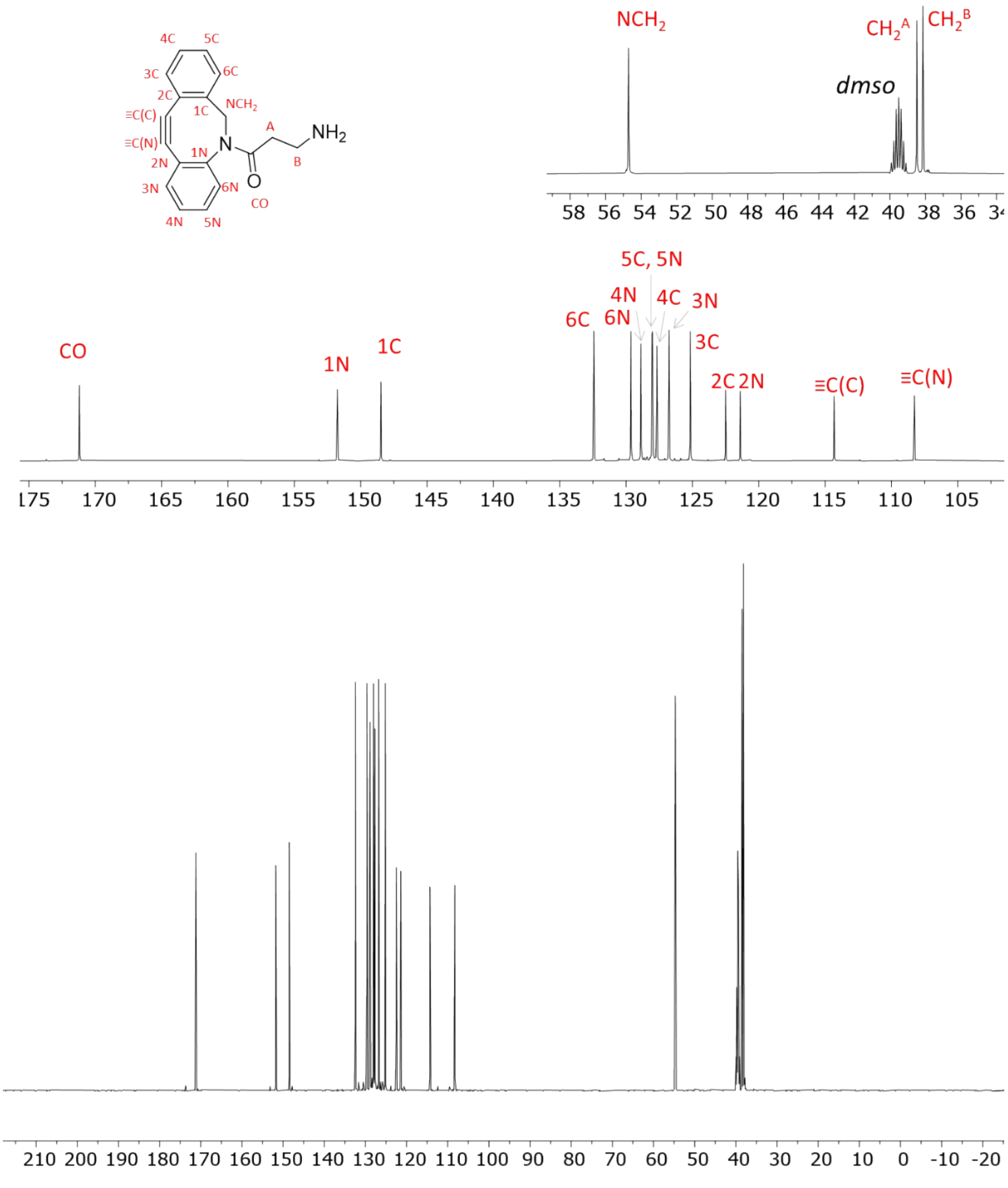

$^{13}C\{^1H\}$ NMR (d_6-DMSO, 151 MHz, 293 K): 171.2 (CO), 151.8 (C^{1N}), 148.5 (C^{1C}), 132.4 (CH^{6C}), 129.6 (CH^{6N}), 128.9 (CH^{4N}), 128.0 (CH^{5C}), 128.0 (CH^{5N}), 127.8 (CH^{4C}), 126.8 (CH^{3N}), 125.5 (CH^{3C}), 122.5 (C^{2C}), 121.4 (C^{2N}), 114.3 (≡C(C)), 108.3 (≡C(N)), 54.7 (NCH_2^{DBCO}), 38.5 (CH_2^A), 38.1 (CH_2^B).

Figure S7. ^{1}H NMR (d_6-DMSO, 600 MHz, 293K) spectrum of **2**.

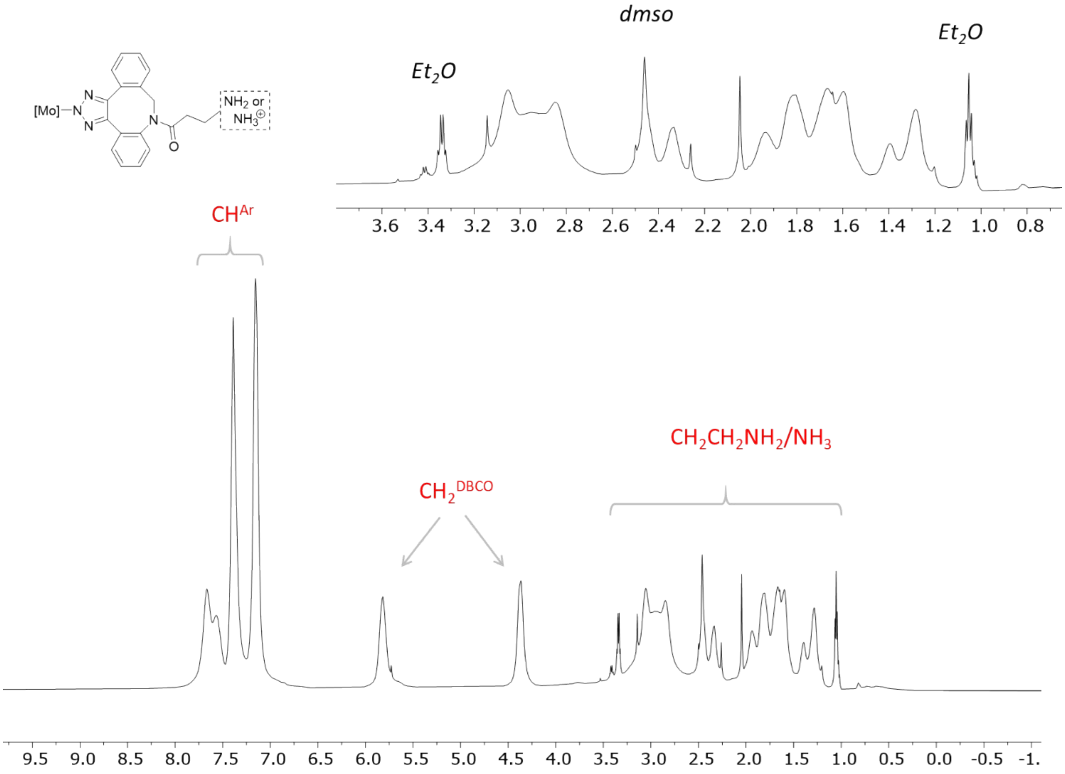

NMR analysis showed two organic fragments in cca 2:1 ratio. ^{1}H and ^{13}C{^{1}H} NMR shifts were similar in the aromatic region, with a notable difference mainly for the amine-substituted pendant arm. This suggests that **2** contains two protonated amine groups and exhibits zwitterionic character in solution. As a result, we report the chemical shifts only for the characteristic moieties.

^{1}H NMR (d_6-DMSO, 600 MHz, 293 K) selected resonances: [7.67, 7.56, 7.39, 7.15](all br, CH^{Ar}), [5.82, 4.38](br s, CH$_2$N^{DBCO}).

Figure S8. $^{13}C\{^{1}H\}$ NMR (d_6-DMSO, 151 MHz, 293 K) spectrum of **2**.

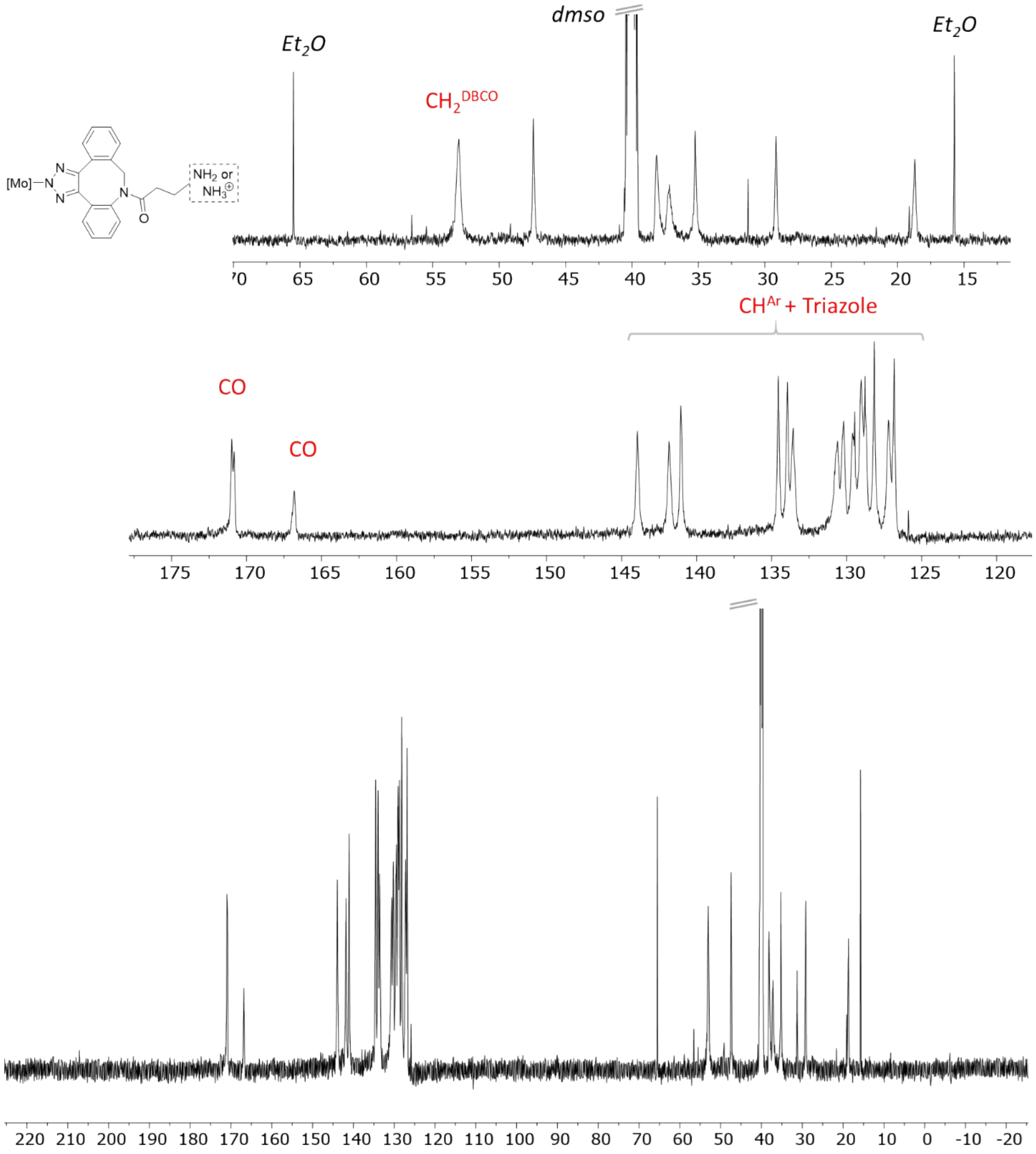

NMR analysis showed two organic fragments in cca 2:1 ratio. ^{1}H and $^{13}C\{^{1}H\}$ NMR shifts were similar in the aromatic region, with a notable difference mainly for the amine-substituted pendant arm. This suggests that **2** contains two protonated amine groups and exhibits zwitterionic character in solution. As a result, we report the chemical shifts only for the characteristic moieties.

$^{13}C\{^{1}H\}$ NMR (d_6-DMSO, 151 MHz, 293 K): [171.0, 166.8](CO-amide), 53.1 [CH_2N^{DBCO}].

Figure S9. ^{1}H NMR (d_6-DMSO, 600 MHz, 293K) spectrum of m-dPEG®12-DBCO.

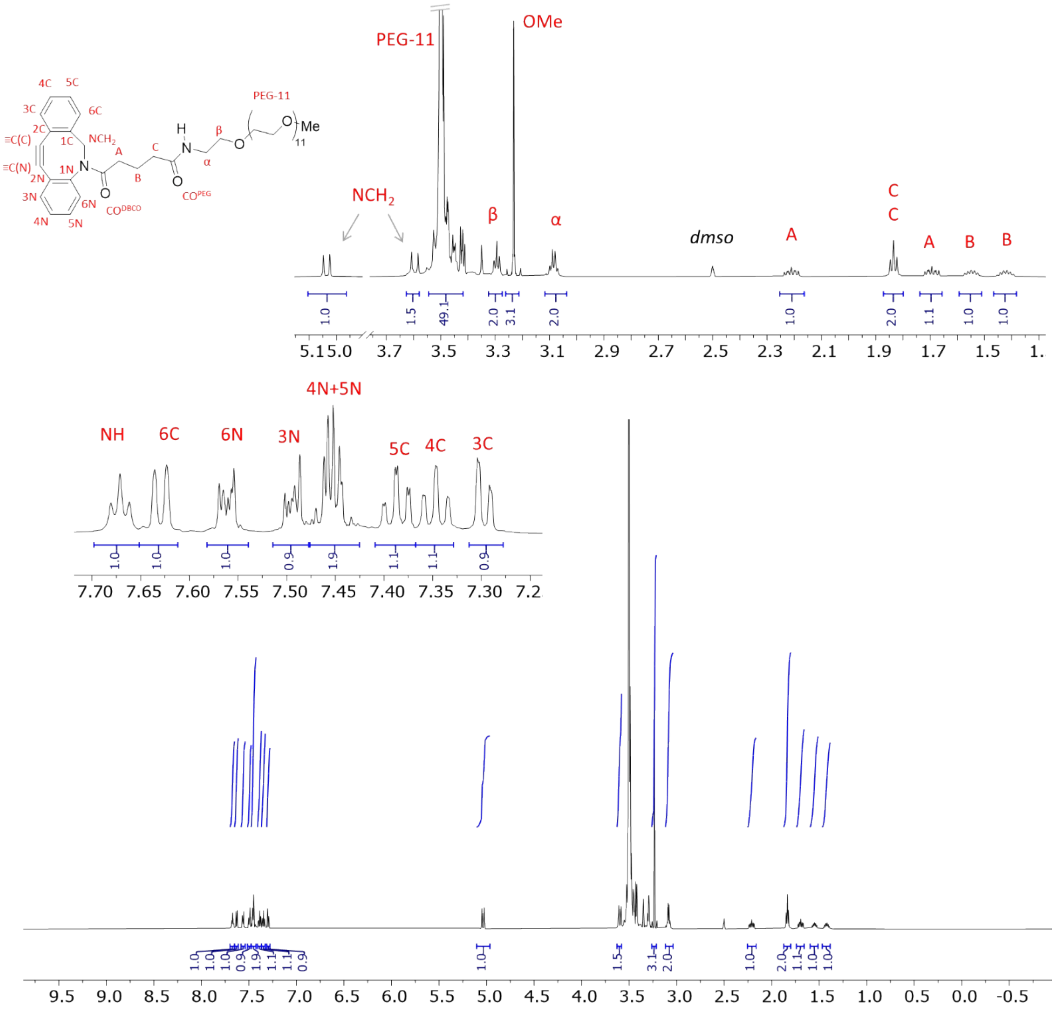

^{1}H NMR (d_6-DMSO, 600 MHz, 293 K): 7.67 (t, $^3J_{HH}$ = 5.7 Hz, 1H, NH), [7.63 (dd, $^3J_{HH}$ = 7.5 Hz, $^4J_{HH}$ = 1.3 Hz, 1H, CH^{6C}), 7.56 (m, 1H, CH^{6N}), 7.49 (m, 1H, CH^{3N}), 7.46-7.44 (m, 2H, CH^{4N+5N}) 7.39 (ddd, $^3J_{HH}$ = $^3J_{HH}$ = 7.5 Hz, $^4J_{HH}$ = 1.4 Hz, 1H, CH^{5C}), 7.35 (dd, $^3J_{HH}$ = $^3J_{HH}$ = 7.5 Hz, $^4J_{HH}$ = 1.3 Hz, 1H, CH^{4C}), 7.30 (dd, $^3J_{HH}$ = 7.5 Hz, $^4J_{HH}$ = 1.4 Hz, 1H, CH^{3C})](CH^{Ar}), [5.04 (d, $^2J_{HH}$ = 14.1 Hz), 3.60 (d, $^2J_{HH}$ = 14.1 Hz)](each 1H, NCH$_2^{DBCO}$), 3.35-3.40 (m, PEG-11), 3.29 (t, $^3J_{HH}$ = 6.0 Hz, 2H, CH$_2^{\beta}$), 3.23 (s, 3H, OMe), 3.08 (dt, $^3J_{HH}$ = $^3J_{HH}$ = 6.0 Hz, 2H, CH$_2^{\alpha}$), 2.21 (m , 1H, CH$_2^{A}$), 1.81 (m, 2H, CH$_2^{C}$), 1.69 (m , 1H, CH$_2^{A}$), 1.55 (m , 1H, CH$_2^{B}$), 1.42 (m , 1H, CH$_2^{B}$).

Figure S10. $^{13}C\{^{1}H\}$ NMR (d_6-DMSO, 151 MHz, 293 K) spectrum of m-dPEG®12-DBCO.

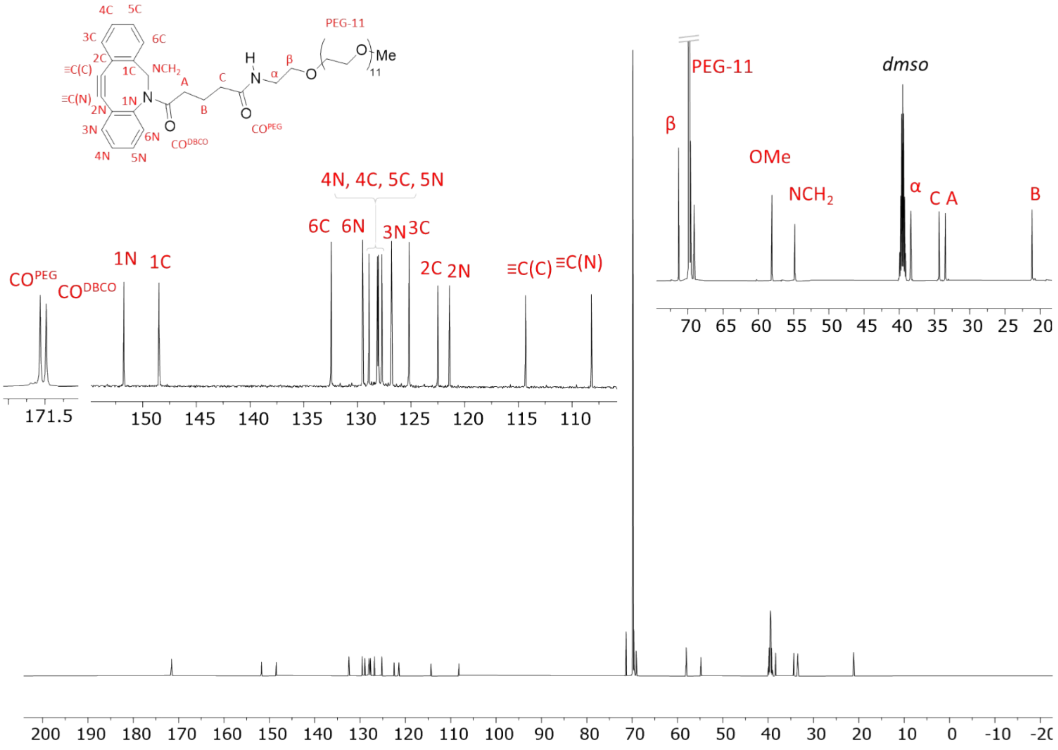

$^{13}C\{^{1}H\}$ NMR (d_6-DMSO, 151 MHz, 293 K): 171.6 (CO^{PEG}), 171.5 (CO^{DBCO}), 151.8 (C^{1N}), 148.5 (C^{1C}), 132.5 (CH^{6C}), 129.5 (CH^{6N}), [128.9, 128.1, 128.0, 127.7](CH^{4N}, CH^{4C}, CH^{5C}, CH^{5N}), 126.8 (CH^{3N}), 125.5 (CH^{3C}), 122.5 (C^{2C}), 125.2 (C^{2N}), 114.3 (≡C(C)), 108.2 (≡C(N)), 71.3 (CH$_2^{\beta}$), 69.8 (PEG-11), 58.1 (OMe), 54.8 (NCH$_2^{DBCO}$), 38.4 (CH$_2^{\alpha}$), 34.4 (CH$_2^{C}$), 33.5 (CH$_2^{A}$), 23.2 (CH$_2^{B}$).

Figure S11. ^{1}H NMR (d_6-DMSO, 600 MHz, 293K) spectrum of **3**.

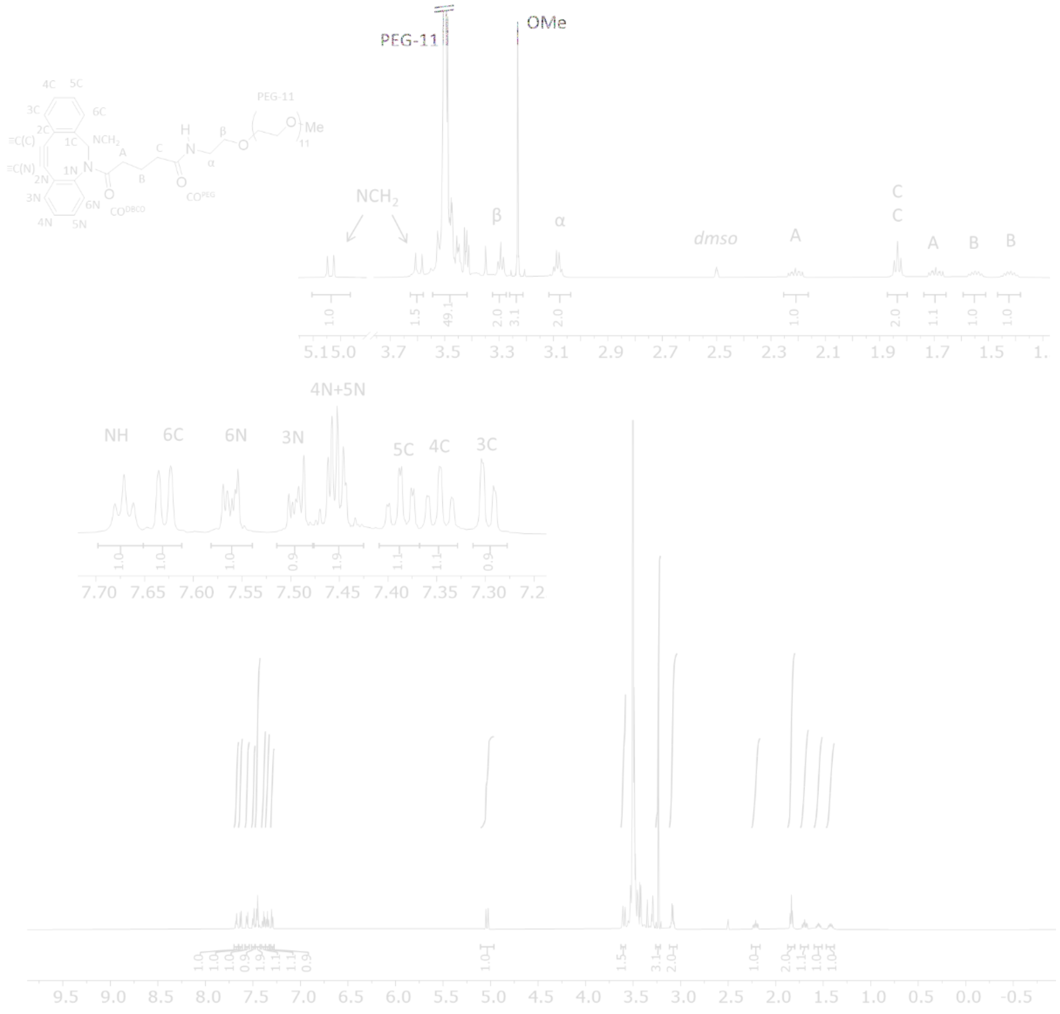

^{1}H NMR (d_6-DMSO, 600 MHz, 293 K) selected resonances: 7.67 (br, 1H, NH), 7.72-7.49 (m, 2H, CH^{Ar}), 7.45-7.32 (m, 3H, CH^{Ar}), 7.21-7.11 (m, 3H, CH^{Ar}), 5.82 (br, 1H, NCH_2^{DBCO}), 4.37 (br, 1H, NCH_2^{DBCO}), 3.53-3.33 (m, PEG-11), 3.22 (s, 3H OMe), 3.02 (br, 2H, CH_2^{α}), [1.89, 1.80, 1.71, 1.55, 1.54, 1.30](each br, 1H, CH_2^{ABC}).

Figure S12. ^{13}C{^{1}H} NMR (d_6-DMSO, 151 MHz, 293 K) spectrum of **3**.

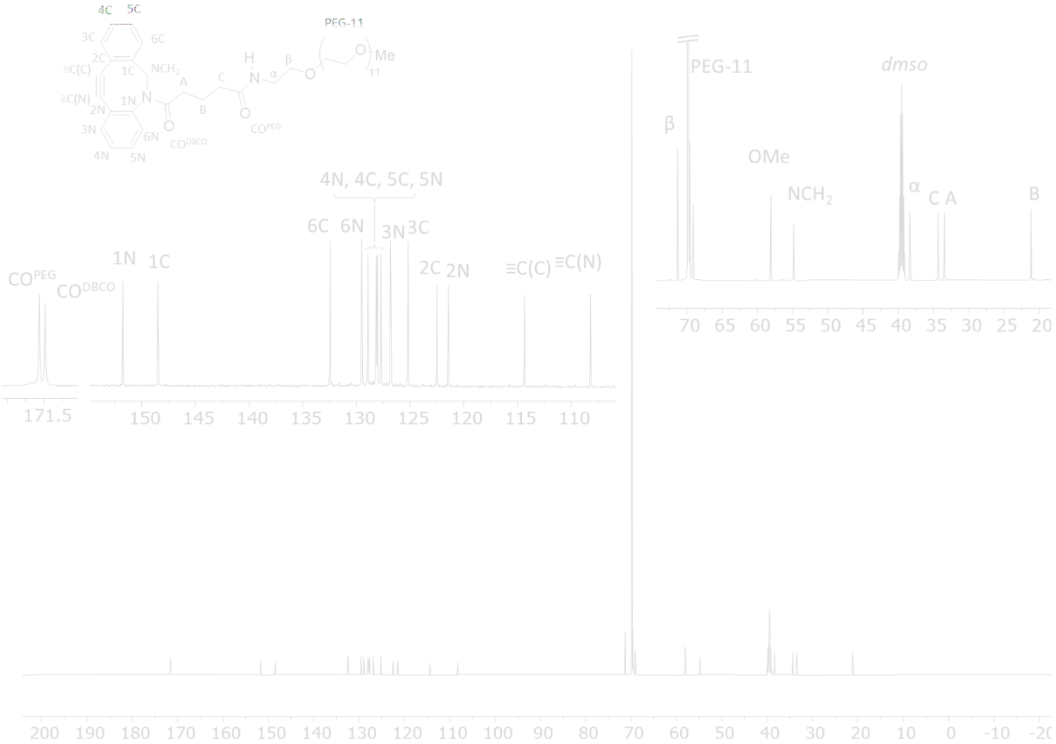

^{13}C{^{1}H} NMR (d_6-DMSO, 151 MHz, 293 K): [171.1, 171.0](CO), [143.4 (m), 141.3 (m)](C-triazole), [140.5, 134.0, 133.4, 133.0, 130.1, 129.8, 129.0, 128.5, 128.2, 127.5, 126.6, 126.3](C^{Ar} and CH^{Ar}), 71.3 (CH$_2^{\beta}$), 69.8 (PEG-11), 58.1 (OMe), 52.7 (NCH$_2^{DBCO}$), 38.3 (CH$_2^{\alpha}$), 34.4 (CH$_2^{A/C}$), 32.2 (CH$_2^{A/C}$), 20.6 (CH$_2^{B}$).

Figure S13. High resolution mass spectroscopy of **1**, **2**, and **3** in the negative mode (black) with corresponding calculated mass spectra (red).

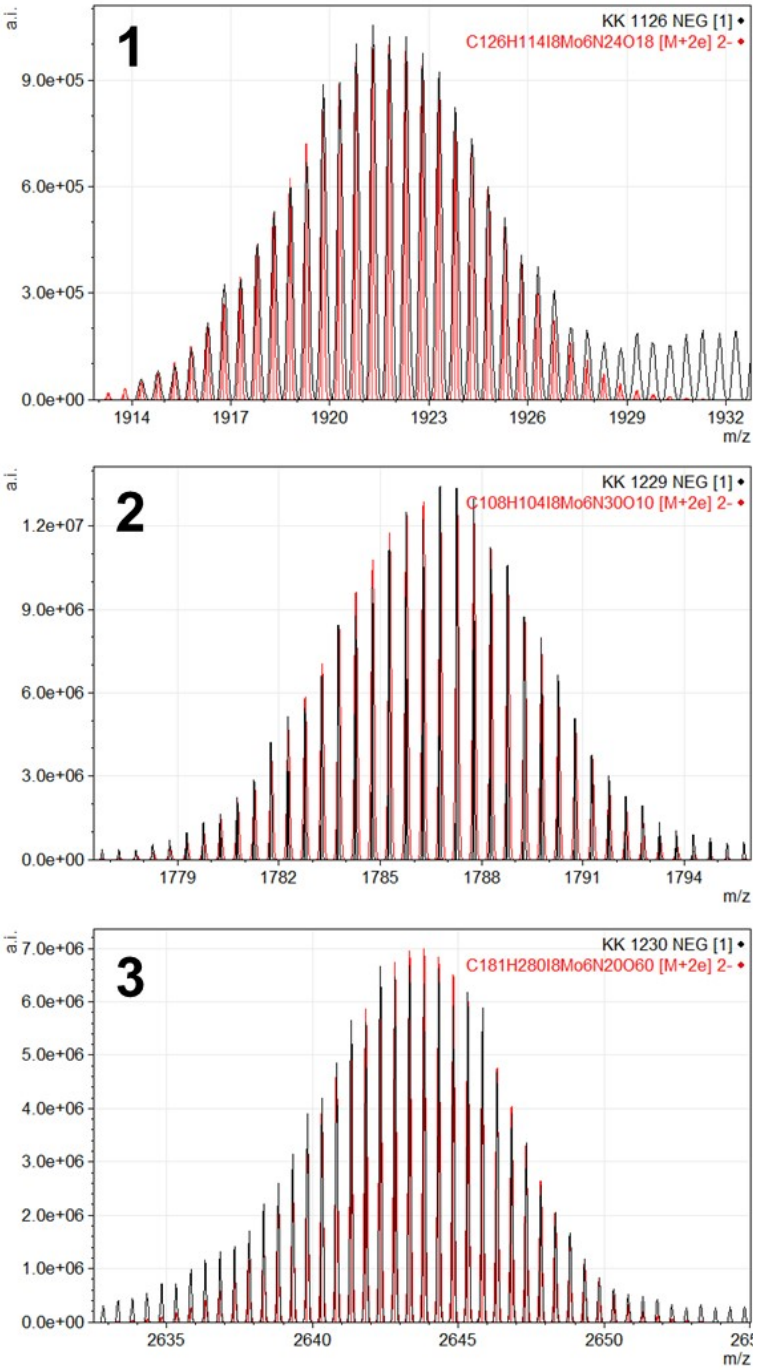

Figure S14. Size distribution by intensity of deionized water and PBS dispersions of **1**, **2**, and **3**.

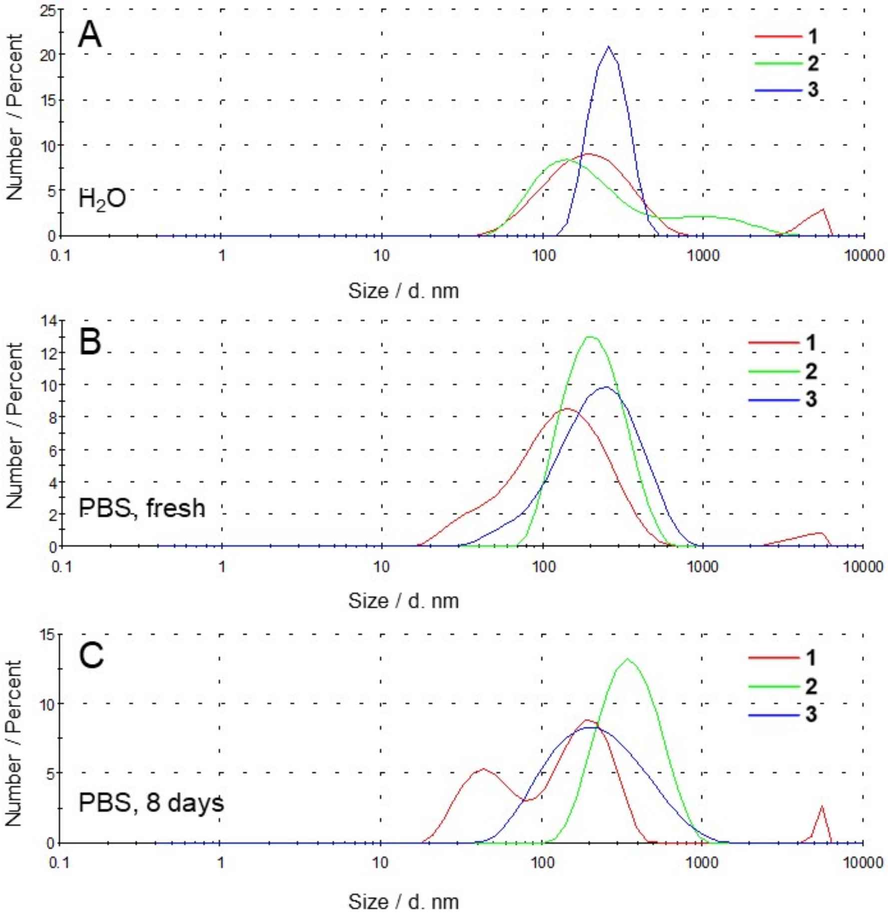

Figure S15. Zeta potentials of aqueous dispersions of **1**, **2**, and **3** from pH~4 to pH~8.

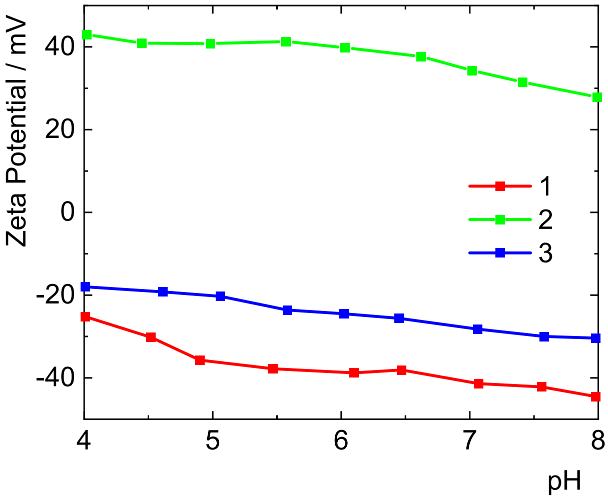

Figure S16. Phosphorescence and radioluminescence of the solid samples of **1**, **2** and **3** after excitation with 400 nm light and X-rays, respectively. Time-resolved phosphorescence of **1**, **2** and **3** in the solid state in air atmosphere, λ_{ex} = 405 nm, λ_{em} = 700 nm.

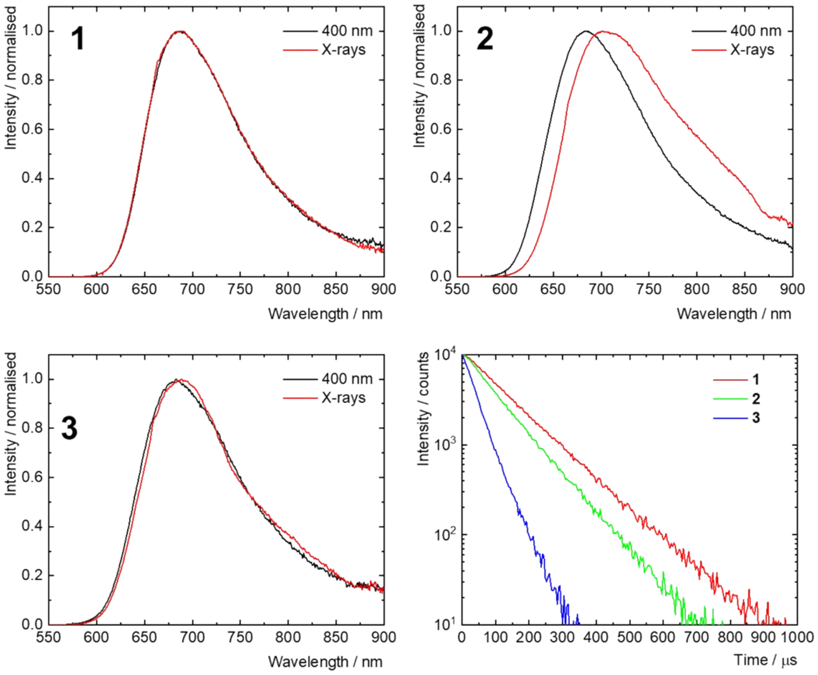

Figure S17. Phosphorescence spectra of fresh and illuminated (460 nm, 15 min, 18 mW cm^{-2}) air-saturated PBS dispersions of **1**, **2**, and **3**.

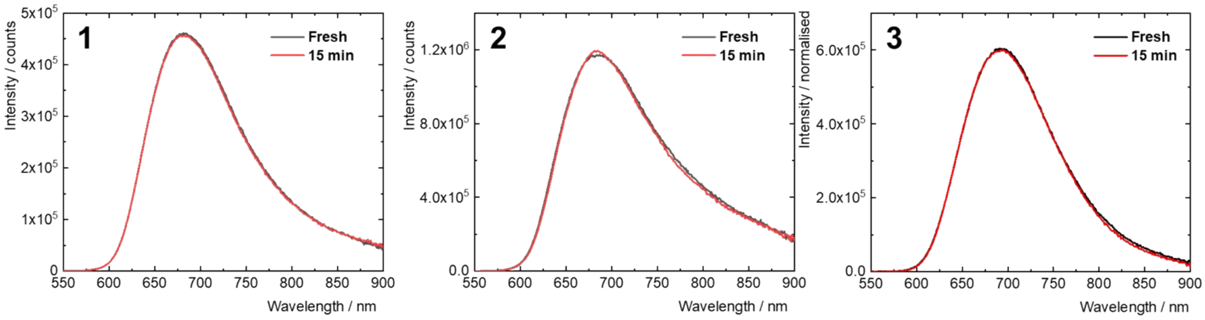

Figure S18. Normalized phosphorescence spectra of fresh (black) and 8-days old (red) argon-saturated PBS dispersions of **1**, **2**, and **3,** λ_{ex} = 400 nm.

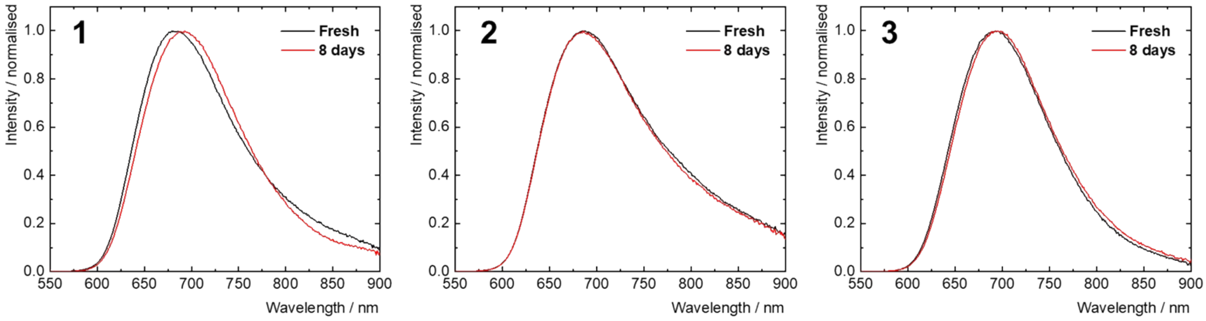

Figure S19. Phosphorescence decay kinetics of fresh (black) and 8-days old (red) dispersions of **1**, **2**, and **3** in argon-saturated (full line) or air-saturated (dashed line) PBS, λ_{ex} = 405 nm, λ_{em} = 700 nm.

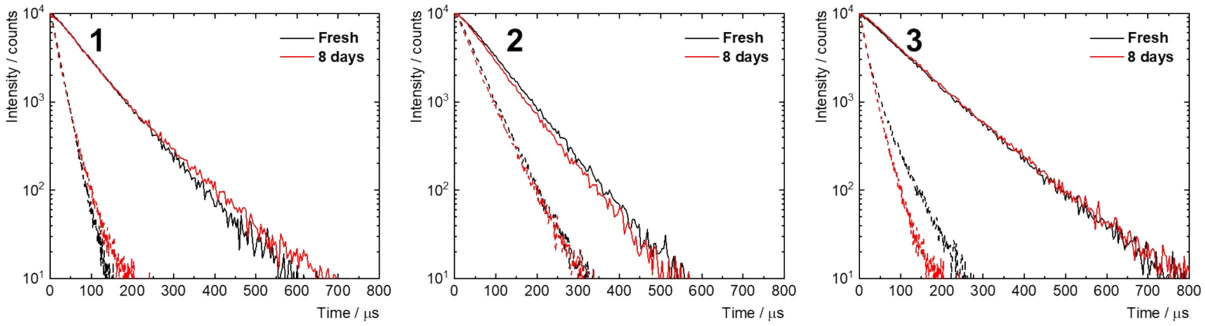

Figure S20. Effect of compounds **1**, **2**, and **3** after 2h incubation with HeLa cells in the FBS-free medium (**A**) illuminated with blue light (460 nm, 15 min, 18 mW cm^{-2}) or (**B**) kept in the dark.

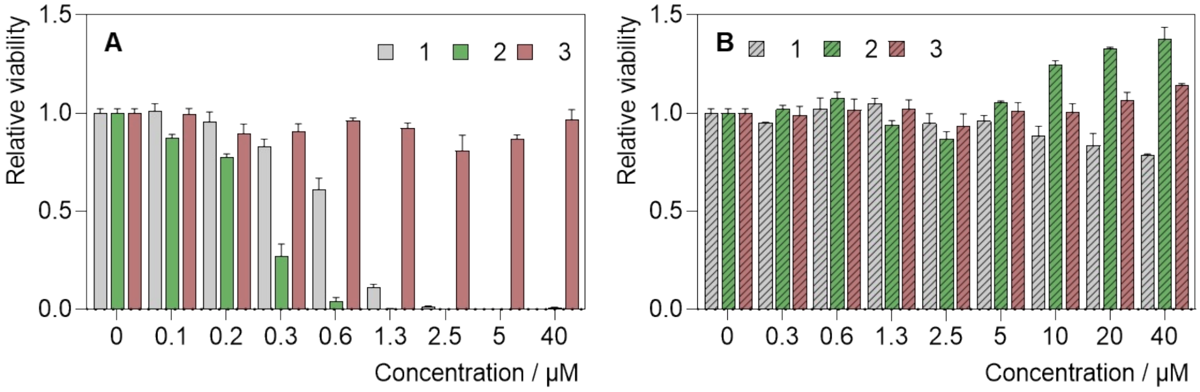

Figure S21. Effect of compounds **1**, **2**, and **3**, aged in water/DMSO mixture (1:9, v/v) for 8 days, after 2h incubation with HeLa cells in the full medium (**A**) illuminated with 460 nm light (460 nm, 15 min, 18 mW cm^{-2}) or (**B**) kept in the dark.